Spatial Properties of Photophobia

James M. Stringham,[1,2] *Kenneth Fuld,*[2] *and Adam J. Wenzel*[2]

Purpose. To determine the spatial properties of stimuli that elicit photophobia (PP) in normal subjects: Does PP exhibit spatial summation? Are different parafoveal quadrants (superior, inferior, temporal, and nasal) of the retina differentially sensitive in PP? What is the relationship between PP sensitivity and retinal eccentricity? What is the relationship between the spatial properties of PP and the spatial distribution of macular pigment (MP)?

Methods. A Maxwellian-view optical system with a xenon light source was used to present the stimuli. Four normal subjects viewed stimuli of various sizes, retinal locations, and one of two chromatic contents: xenon-white and a broadband orange. The intensity of the test stimulus was increased between trials until the PP threshold was reached. The squinting response corresponding to PP was assessed by electromyography and used as an objective criterion of PP. Three parameters were examined: stimulus size, parafoveal retinal locus (superior, inferior, temporal, and nasal), and retinal eccentricity (extending into the perifovea). Spatial profiles of MP were measured psychophysically using heterochromatic flicker photometry (HFP).

Results. Spatial summation for PP was found essentially to adhere to Piper's law (radiance proportional to square root of stimulus area). The PP response was greater to centrally than peripherally viewed targets. In this regard, MP acted as a spatially integrated filter in the attenuation of PP.

Conclusions. The degree of spatial summation found for PP indicates that an increase of 1.0 log unit in field area results in an approximately 0.57-log-unit decrease in the radiance required to elicit PP. PP appears to serve the function of retinal photoprotection. (*Invest Ophthalmol Vis Sci.* 2004;45: 3838–3848) DOI:10.1167/iovs.04-0038

Photophobia (PP), the clinical term for light-induced visual discomfort, is a common symptom of various ocular and brain-related maladies such as corneal abrasion, iritis,[1] tumors compressing the anterior visual pathways,[2] trigeminal neuralgia,[3] and, perhaps most prominently, migraine headache.[4,5] Although PP is usually thought of as coinciding with disease, it is a common phenomenon experienced by anyone who has ever entered a lighted environment that is subjectively appraised as "too bright" to tolerate, requiring an aversive response of some sort. For the purposes of this study, we define PP as light-induced visual discomfort that is indicated by a sufficient squinting response (discussed in the Methods section).

The neurophysiological processes that give rise to PP are poorly understood. Because pain-signaling fibers of the trigeminal nerve innervate the dilator and constrictor muscles of the iris, it has been suggested that the pupillary light reaction could give rise to PP under lighting conditions that cause intense stretching and maximum constriction of the irides.[6] Indeed, it has been demonstrated that an intact trigeminal nerve is necessary to experience PP.[7] More recently, however, it has been shown that hippus (an irregular oscillation of iris constriction and dilation under intense illumination) is not consistently associated with subjective reports of visual discomfort.[8] Moreover, the finding of binocular summation in visual discomfort[9–11] contradicts the suggestion of the pupil response as a PP mechanism, given the well-known consensual light reflex. In other words, for monocular viewing of a PP-inducing stimulus, both pupils constrict approximately equally, yet more light is needed to elicit PP than for binocular viewing. PP, therefore, appears to have a central nervous system component.

Using a criterion squinting response as a measure of PP, Stringham et al.[12] found that, unlike common spectral sensitivity functions (e.g., $V(\lambda)$ and $V'(\lambda)$), the action spectrum for PP, after correction for ocular media and macular pigment absorption, exhibits increasing sensitivity with decreasing wavelength. It is a well-established fact that the energy value per quantum of light is inversely related to wavelength. Thus, shorter wavelengths contain more energy and are potentially more damaging to biological tissue. Based on this idea, Stringham et al.[12] have proposed that the PP action spectrum is indicative of an increased sensitivity to potentially damaging short-wavelength light. Other experimental results are consistent with this conclusion. Ham et al.[13] found that the threshold energy for retinal damage decreased with reduction of wavelength in the rhesus macaque, in a fashion similar to the corrected-action spectrum for PP of Stringham et al.[12] In addition, the same type of relationship has been established for threshold retinal damage in the rat.[14] It follows that an aversive response (squinting), biased toward the short wavelengths, would serve a function of biological protection.

Beyond the PP action spectrum of Stringham et al.,[12] little is known about how basic stimulus parameters affect PP in normal subjects. Although the spatial properties for many aspects of vision have been well established (e.g., contrast sensitivity,[15] threshold summation,[16] and detection as a function of eccentricity[17]), a comprehensive, detailed assessment of the spatial properties of PP has yet to be performed. The questions addressed in the present investigation were: What is the relationship between stimulus area, energy content of the stimulus, and threshold PP for centrally viewed stimuli? Does the threshold for PP change with respect to the region (i.e., nasal, temporal, superior, and inferior) of the retina stimulated? Does the PP threshold change with increasing retinal eccentricity? Is there a relationship between the spatial properties of the threshold PP response and the spatial distribution of macular pigment (MP) in the retina?

From the [1]Department of Ophthalmology, Medical College of Georgia, Augusta, Georgia; and the [2]Department of Psychology, University of New Hampshire, Durham, New Hampshire.

This article presents findings from James M. Stringham's doctoral dissertation research, which was conducted at the University of New Hampshire.

JMS was supported in part by the Gustavus and Louise Pfeiffer Research Foundation.

Submitted for publication January 14, 2004; revised July 1, 2004; accepted July 15, 2004.

Disclosure: **J.M. Stringham**, None; **K. Fuld**, None; **A.J. Wenzel**, None

The publication costs of this article were defrayed in part by page charge payment. This article must therefore be marked "*advertisement*" in accordance with 18 U.S.C. §1734 solely to indicate this fact.

Corresponding author: James M. Stringham, Department of Psychology, University of Georgia, Psychology Building, Room 215, Baldwin Street, Athens, GA 30602-3013; psychjim@uga.edu.

Investigative Ophthalmology & Visual Science, October 2004, Vol. 45, No. 10
Copyright © Association for Research in Vision and Ophthalmology

Downloaded from iovs.arvojournals.org on 06/13/2021

METHODS

Subjects

Three men, 25, 32, and 30 years of age, and one woman, 34 years of age, served as subjects for this study. One of the men (subject VH), participated in three of the four experiments within the study. All subjects underwent standard visual perimetric assessment (Octopus perimeter; Interzeag Co., Köniz-Berne, Switzerland) to confirm normal visual fields and to document the exact location, size, and shape of each subject's blind spot. None of the subjects had a history of visual disease. All experimental procedures adhered to the tenets of the Declaration of Helsinki. Informed consent was obtained from the subjects after explanation of the nature and possible consequences of the study. This study was approved by the University of New Hampshire's institutional review board and the Medical College of Georgia's Human Assurance Committee.

Apparatus

A three-channel standard Maxwellian-view system with a 1000-W xenon arc lamp was used. In one channel, a xenon-white, 30.5°, mesopic level (0.1 cd/m^2) background field served to maintain subjects' adaptation level before presentation of the test stimulus. The second channel was used to present a 20-minarc, red fixation point. The third channel provided the test stimulus, either a xenon-white or orange disc of light ranging from 5.6° to 28.3° of visual angle, depending on the experiment. The orange stimulus was created by passing xenon-white light through a long-pass optical filter (no. 15; Tiffen Manufacturing Corp, Hauppauge, NY), which turns on at approximately 540 nm. Because macular pigment absorbs light from approximately 400 to 530 nm, use of this filter for producing PP precluded effects of macular pigment absorption. Neutral-density filters and a neutral-density wedge were used to adjust the intensity of the test stimulus. The diameter of the xenon arc image conjugate with the pupil was 1.25 mm. PP-inducing energy levels were measured after each session with a radiometer (Optometer 61; United Detector Technology, Hawthorne, CA).

A criterion squinting response, measured with an electromyogram (EMG), served as the operational definition of threshold PP. This method had yielded reliable results in a previous study.[12] For assessing subjects' squinting responses, an EMG preamplifier/amplifier (model 7P3B; Grass-Telefactor, Inc., West Warwick, RI), routed through a signal integrator, was coupled to one channel of a computer-based waveform analyzer/recorder. For precise determination of the portion of the recording that corresponded to stimulus presentation, the switch used to open and close the test-channel shutter was wired to send a pulse to the second channel of the computer.

Procedure

In experiment 1, we assessed the PP threshold for centrally viewed white or orange stimuli that varied in size from trial to trial. The test stimuli were concentric with the background field. The dimly lit red fixation point remained in the center of the background field, to ensure central viewing of the test field. For experiment 2, which we used to assess PP thresholds to a 5.6° stimulus in the parafovea of nasal, temporal, superior, and inferior retina, the fixation point was positioned in a location that allowed for placement of the test field in the retinal region of interest. For example, for the test stimulus to appear in the inferior retina, the fixation point was placed tangential to the lower rim of the test stimulus. For experiment 3, in which we assessed PP thresholds to a 9.5° stimulus viewed centrally and at two peripheral locations (10° and 20°) in the temporal retina, the fixation point was placed at the desired distance to the right of the test stimulus.

To ensure a subject's stable alignment with the optical system, a dental impression bite bar and forehead stabilizers were used. A pupillary alignment procedure was performed to confirm that the light from the optical system was in focus in the plane of the subject's pupil and passing through the center of the subject's pupil. Initially, the subjects were dark adapted for 15 minutes. The background field was then presented, and the subject was instructed to fixate the fixation point placed in the center of the background field (experiment 1), or in one of four (right, left, top, bottom) tangential test field locations (experiment 2), or in a 10° or 20° location to the right of the center of the to-be-viewed test stimulus (experiment 3). After 1 minute, the subject was presented with the test stimulus for 5 seconds. The two shutters in the optical system were wired out of phase with respect to each other, which allowed for an exact exchange of the background and test fields. The background field subtended 30.5°, and the test stimuli (experiment 1) were one of eight sizes: 5.6°, 6.8°, 8.2°, 9.5°, 12.4°, 16.9°, 22.3°, or 28.3°. The background field was therefore always larger than the test stimulus, by at least 2.2°. Cornsweet[18] showed that, during fixation, minor involuntary eye drifts do not exceed 6.6 minarc of visual angle. Glezer[19] found the maximum drift angle during fixation to be approximately 10 minarc. Therefore, in the case of minor drifting eye movements, the larger background field in the present study ensured an equal adaptation of the retinal area to be stimulated by the test field. This arrangement also ensured that, while viewing the test stimulus, a subject's minor eye movements would not train the test stimulus onto an area of the retina that was outside the 30.5° subtense of the background–adaptation field and therefore more dark adapted. In subsequent trials, the subject was dark adapted for approximately 10 minutes after the test and was then instructed to view the mesopic-level background. The background was flashed on and off by the experimenter, and the subject was asked whether a residual afterimage from the previous trial was present. The perception of an afterimage necessitated additional dark adaptation to reach the mesopic threshold. At the point when no afterimage was present, the procedure, as described earlier, continued.

PP was assessed by recording the muscle potentials associated with subjects' squinting responses by EMG. Surface electrodes were at-

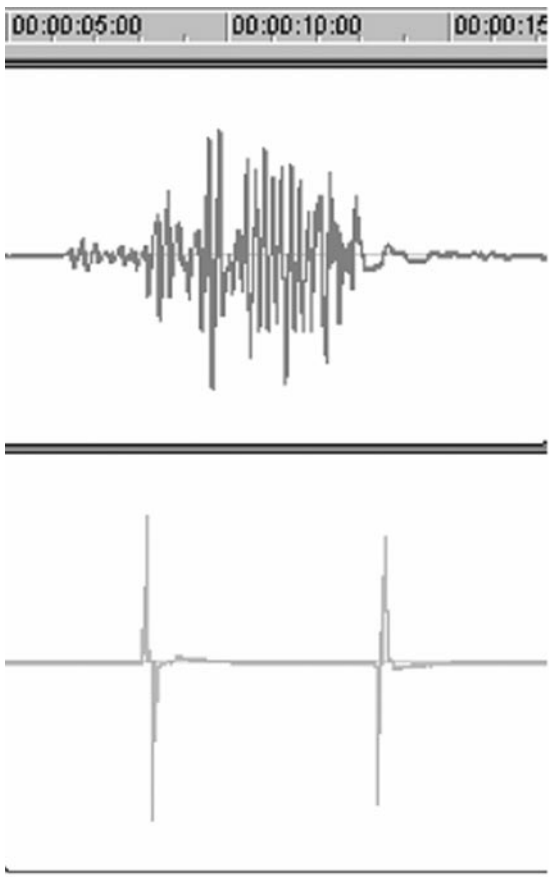

FIGURE 1. *Top*: typical EMG of threshold PP squinting response. *Bottom*: spikes corresponding to onset and termination of test stimulus.

Downloaded from iovs.arvojournals.org on 06/13/2021

tached to the right temple (reference), to the upper cheek, below the lateral canthus of the right eye (test), and on the back of the neck (ground). The EMG was used solely for the determination of a threshold PP response. The criterion threshold PP response was based on the amplitude and duration of squint. A continuous squint response that lasted at least one half the duration of the test stimulus presentation and that reached a 4:1 signal-to-noise ratio (squinting activity/baseline) at any point during the continuous squinting was considered a threshold PP response. These criteria were determined to correlate strongly with the subjective experience of discomfort during preliminary testing.

We have found that a subject often blinks or exhibits a "startle squint" on presentation of the test stimulus, followed by normal fixation or some squinting (depending on the discomfort caused by the test stimulus) for the remainder of the stimulus presentation. This startle reaction is the well-known photic startle response.[20] On traces where the photic startle response was evident, neither its amplitude nor its duration was factored into the PP threshold criteria. Figure 1 shows an example of a typical criterion PP response.

The method of ascending limits was used for all the experiments. A relatively low-intensity test stimulus was initially presented, and, in steps separated by dark adaptation, the intensity of the stimulus was increased, in increments of 0.10 log unit, until the PP threshold was reached. The order of presentation with regard to stimulus size and location was randomly determined.

For experiment 1, two sessions (one with the white and one with the orange test field) were necessary to complete assessment at all eight stimulus sizes. In one session (with either the white or orange test field), measurements were made for four stimulus sizes; in the second session, five stimulus sizes were used. To normalize results from the two sessions within each light condition, a PP threshold measure for 9.5° was taken during each session. In this way, any response variability arising from differences in electrode placement, subjects' day-to-day absolute sensitivity, or output of the optical system

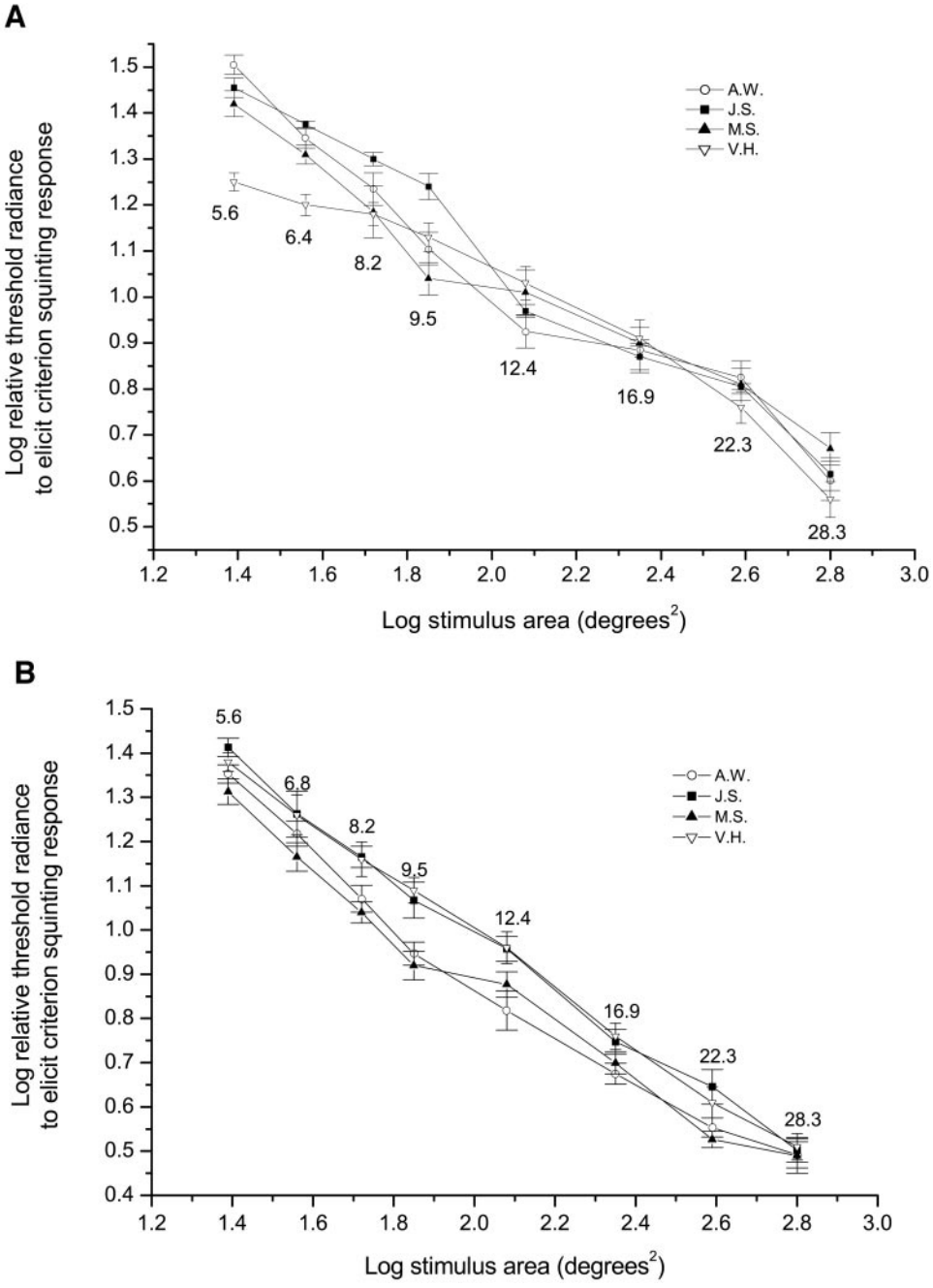

FIGURE 2. **(A)** Log relative radiance thresholds for PP to xenon-white light plotted as a function of log stimulus area. Stimulus diameters are noted near data points. **(B)** Log relative radiance thresholds for PP to orange light plotted as a function of log stimulus area. Stimulus diameters (in degrees of visual angle) are noted near data points.

Downloaded from iovs.arvojournals.org on 06/13/2021

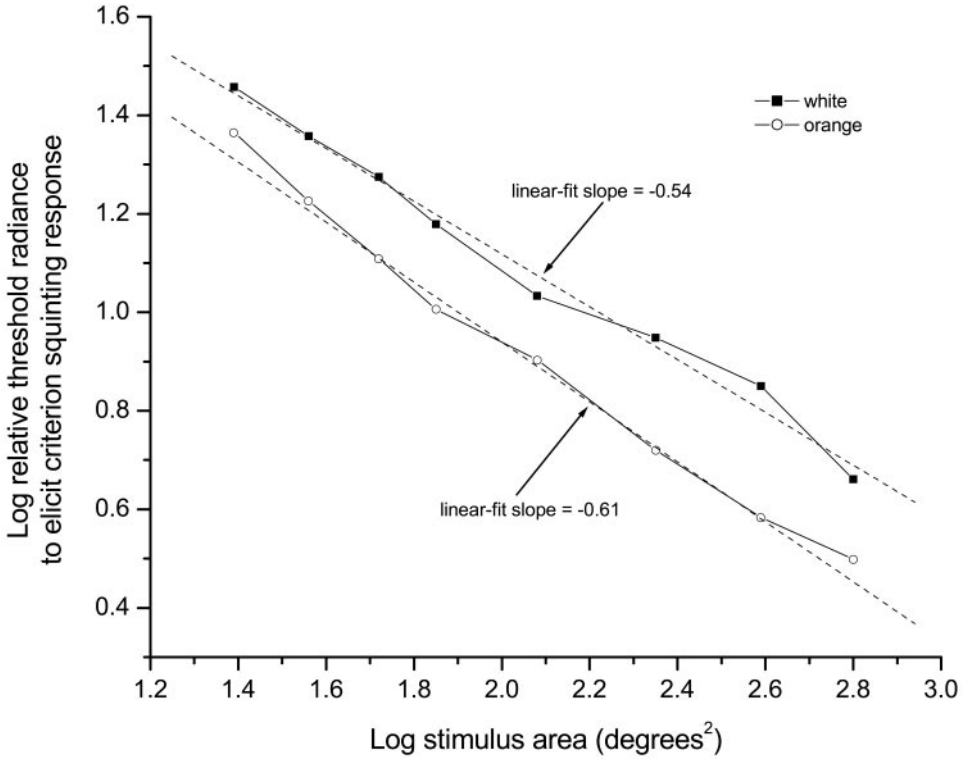

FIGURE 3. Subjects' averaged data for xenon-white and orange conditions, plotted for comparison. Linear fits to the data are plotted through each function. Functions are arbitrarily displaced along the *y*-axis to allow for comparison.

was offset by a scalar shift along the axis of ordinates. Experiments 2 and 3 were each completed in two sessions (one each with white or orange stimuli). All three experiments were repeated a second time in each subject.

Measurement of Macular Pigment

A slightly modified device described by Wooten et al.[21] was used to obtain spatial distribution profiles of MP optical density (MPOD). This device was designed to use heterochromatic flicker photometry (HFP) for measurements of MPOD.[22] A 460 nm light (maximally absorbed by MP) was alternated in square-wave counterphase with a 550 nm light (not absorbed by MP). The task involved minimizing or nulling the perceived flicker in the test stimulus. To do this, the subject adjusted the radiance of the 460-nm light relative to the 550-nm light. The radiances of the 460-nm null flicker settings were compared to those of the null flicker settings made for a retinal locus known to contain very little or no MP (e.g., 7° eccentricity). The log difference in these settings yields a measure of MPOD at the test locus. (For a detailed treatment of the use of HFP to derive MPOD; see Ref. 22.) To determine values for MPOD near the foveal center, we asked subjects to view centrally one of two stimuli, 40 minarc and 60 minarc in diameter. It has been shown that HFP thresholds are largely a function of stimulation by the edges of the test fields used.[23] Thus, the derived MPODs correspond to the retinal loci where the edges of the field are. For example, using a 60-minarc test stimulus that is centrally fixated provides an estimate of MPOD at 30 minarc (the radius of the test field) retinal eccentricity. To obtain MPODs for retinal eccentricities beyond 30 minarc, we used a fixation point placed the desired angular distance from the nearest edge of the flickering disc. Because we wanted to obtain spatial profiles of MPOD, the subjects performed the flicker-nulling task at several retinal loci along the horizontal and vertical meridians. Two sets of MPOD profiles were obtained for each subject, with six measurements taken at each locus per set. The order of retinal locus testing was counterbalanced with respect to session to control for potential order effects. The averaged profiles were compared to the data obtained in experiments 1, 2, and 3 to determine any relationship between the spatial properties of PP and the spatial distribution of MP.

RESULTS

Experiment 1: Spatial Summation and PP

For the xenon-white light condition, subjects' area versus intensity functions are shown in Figure 2A. The data are plotted in log relative radiances and are not normalized. The functions are similar in shape and scale, and the error bars (± 1 SD) indicate low within-subject variability. From Figure 2A, it can be seen that the radiance necessary to induce PP decreased monotonically as the stimulus area increased. In other words, there appeared to be some spatial summation for PP in response to xenon-white light.

For the orange light condition, subjects' area versus intensity functions are shown in Figure 2B. The error bars indicate low within-subject variability. Moreover, there is very little between-subject variability with respect to the shape of the functions. As with the xenon-white condition, a monotonic decrease in slope indicates some spatial summation for PP in response to orange light.

When the subjects' averaged functions for the white and orange light conditions are compared on the same graph (Fig. 3), they are found to be quite similar in shape, and are significantly correlated ($r = 0.99$; $P < 0.01$). When each is fit with a linear function (Fig. 3), the slopes are found to be similar (-0.54 for white and -0.61 for orange). PP to both xenon-white and orange light therefore appears roughly to conform to Piper's law: The intensity of the PP-inducing stimulus is approximately proportional to the square root of its area. For practical purposes, the degree of spatial summation found for PP indicates that increases of 1.0 log unit in field area result in approximately 0.57 log unit decreases in the radiance necessary to elicit PP.

Experiment 2: PP in the Parafovea

Figure 4A graphically depicts the results of experiment 2 for xenon-white light. The three subjects in this experiment ex-

Downloaded from iovs.arvojournals.org on 06/13/2021

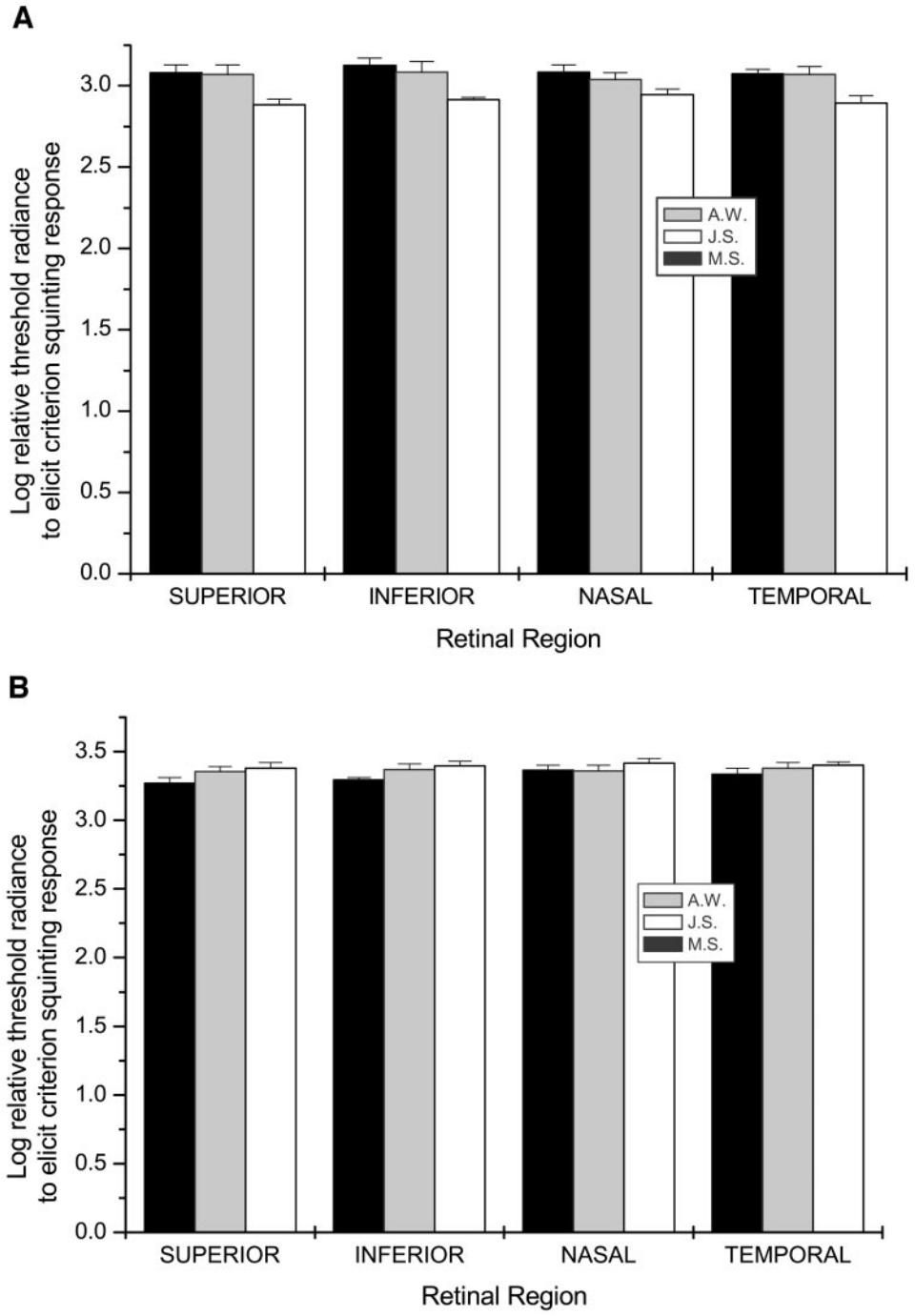

FIGURE 4. **(A)** Log relative radiance thresholds for PP to xenon-white light, plotted as a function of retinal location. **(B)** Log relative radiance thresholds for orange light, plotted as a function of retinal location.

hibited very little within-subject variability in retinal region. At each retinal region tested in subject JS, less energy was needed to elicit a threshold PP response. In contrast, subjects MS and AW were very similar in their radiance requirements to reach PP threshold. A similar lack of within-subject variability was found for the orange-light condition (Fig. 4B). Thus, the PP threshold does not appear to be markedly affected by the different parafoveal retinal locations tested in the present study.

Experiment 3: PP and Retinal Eccentricity

To disentangle the parameters of stimulus size and retinal location, experiment 3 tested PP thresholds to 9.5° discs of xenon-white or orange light at three retinal locations: centrally viewed and at 10° and 20° temporal retinal eccentricity. Results for the xenon-white condition are presented in Figure 5A. At 10° retinal eccentricity, essentially the same radiance as in the central condition was needed in subjects AW and MS to elicit PP, whereas more light was needed in subjects JS and VH, to induce PP at this eccentricity. All subjects showed an increase in PP threshold by 20°.

In the orange-light condition (Fig. 5B), the results for the four subjects bear considerable similarity to one another. All four subjects' radiance thresholds ascend nearly linearly as a function of retinal eccentricity. In addition, the slopes of the four functions are practically identical.

Downloaded from iovs.arvojournals.org on 06/13/2021

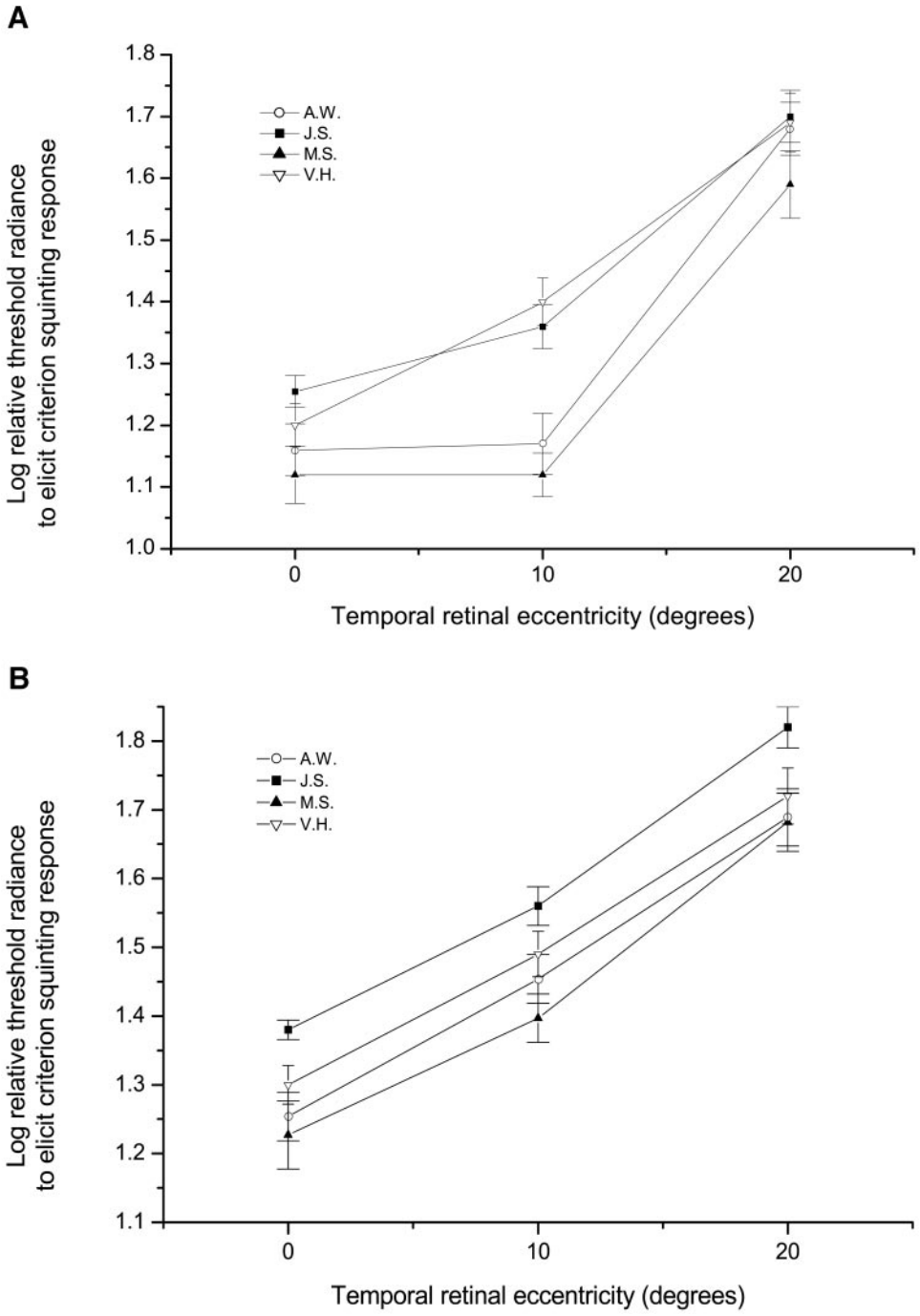

FIGURE 5. **(A)** Log relative radiance thresholds for PP to xenon-white light, plotted as a function of temporal retinal eccentricity. **(B)** Log relative radiance thresholds for PP to orange light, plotted as a function of temporal retinal eccentricity.

Spatial Profiles of MPOD

The subjects' individual spatial distributions of MPOD (averaged from two sessions), along the horizontal and vertical meridians, are plotted in Figure 6. Subject VH was tested along the horizontal meridian only. The data are fit with a Lorentzian function, which fits the actual obtained data well and makes reasonable estimates of the distribution peak. The parameters of the Lorentzian distribution are similar to those of a Gaussian distribution. The Lorentzian distribution is described by the following equation:

$$y = y_0 + \frac{2 \cdot A}{\pi} \cdot \frac{w}{4(x - x_0)^2 + w^2}$$

where y_0 is baseline offset (ordinate value of the curve's asymptote); A is the total area under the curve from the baseline; x_0 is the center of the peak; and w is the full width of the peak at half height. A comparison of the Lorentzian fits of the MPOD distribution data for all four subjects are presented in Figure 7. The smallest four stimulus sizes from experiment 1 (spatial summation experiment) are plotted at the top of the graph to give the reader a conception of the relationship between stimulus size and MPOD spatial distribution. Subject AW (Fig. 6A) was found to have the highest peak, followed by subjects MS (Fig. 6B), JS (Fig. 6C), and VH (Fig. 6D). Subject MS was found to have the broadest MPOD distribution of the four subjects tested. The MPOD distributions for all subjects exhibit approximate vertical and bilateral symmetry, which is consis-

Downloaded from iovs.arvojournals.org on 06/13/2021

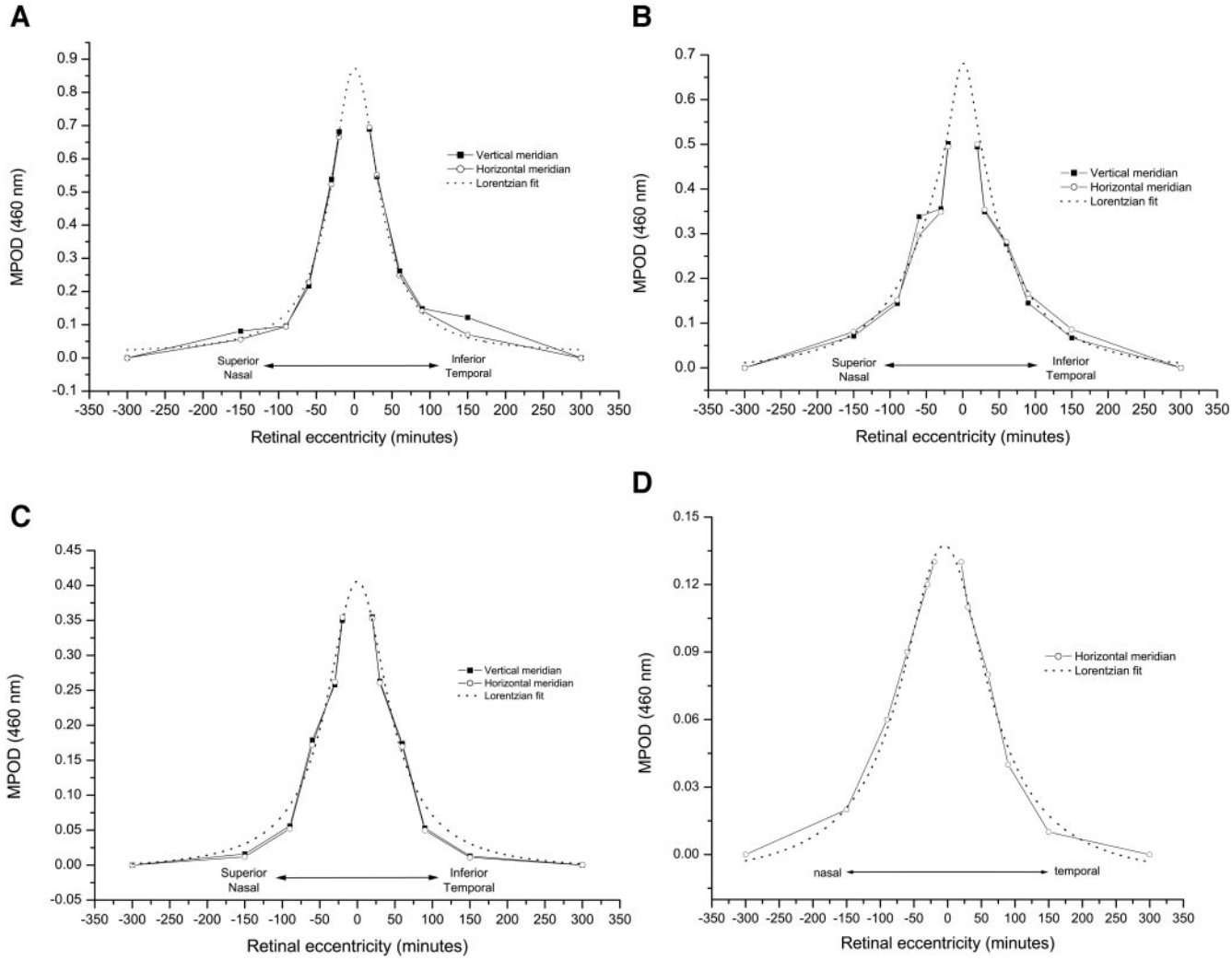

FIGURE 6. Horizontal and vertical meridian spatial profiles of MPOD at 460 nm for subjects AW (**A**), MS (**B**), JS (**C**), and VH (**D**). Lorentzian functions fit to data and plotted for comparison.

tent with previous findings.[24,25] A notable exception to MP's distributional symmetry was a broad "shoulder" found in subject MS's superior retina (Fig. 6B). Subject VH (Fig. 6D) was found to have 0.12 MPOD at 30 minarc eccentricity, which is quite low, even when compared with the lowest published averages.[26]

DISCUSSION

The primary finding of these experiments is that PP exhibits spatial summation for centrally viewed stimuli. For both the xenon-white and orange stimuli, summation for PP appears roughly to follow Piper's law and agrees in this respect with threshold data.[27,28] Although the averaged functions for orange and white light were shown to be similar, there were individual slope differences for the first four data points in the white condition. We speculate that these between-subject slope differences are due to individual differences in MP levels. For example, the first four data points in Fig 2A (representing the four smallest stimuli: 5.6–9.5°) would be those most strongly attenuated by MP, given the spatial distribution of MP (Fig. 7). Stringham et al.[12] showed that short-wavelength light, when corrected for absorption by MP, more readily elicits PP than does long-wavelength light. It could be, therefore, that xenon light (which contains much short-wave energy) is filtered by MP and leads to the increased variability found among our subjects' functions. On an individual basis, subject VH's linear-fit slope for the first four data points is less steep (−0.25) than JS's (−0.47), and considerably flatter than that of either subject AW (−0.85) or subject MS (−0.82). Perhaps the steeper slopes of data for AW and MS are indicative of more heavily weighted screening by their MP for the smaller stimuli. Although there is a marked difference in MPOD spatial profile shape for subjects AW and MS, on integration of MPOD, the values for the two subjects was found to be identical (1.67 log units at 460 nm). Subjects JS and VH were found to have 0.97 and 0.43 log unit integrated MPOD at 460 nm, respectively. The identical integrated MPOD result for subjects AW and MS, coupled with the nearly equivalent slopes for the first four data points in the area versus radiance functions found for these two subjects suggests that the spatial summation in PP is affected by the filtering of an effectively integrated MP. In support of this conclusion, when all four subjects' data were analyzed, a significant correlation between integrated MPODs and linear-fit slopes for the first four data points ($r = -0.99$, $P = 0.003$) was found. Moreover, beyond the 9.5° stimulus, the curves in Figure 2A come together and take on a similar shape, which supports the notion that with relatively large stimulus

Downloaded from iovs.arvojournals.org on 06/13/2021

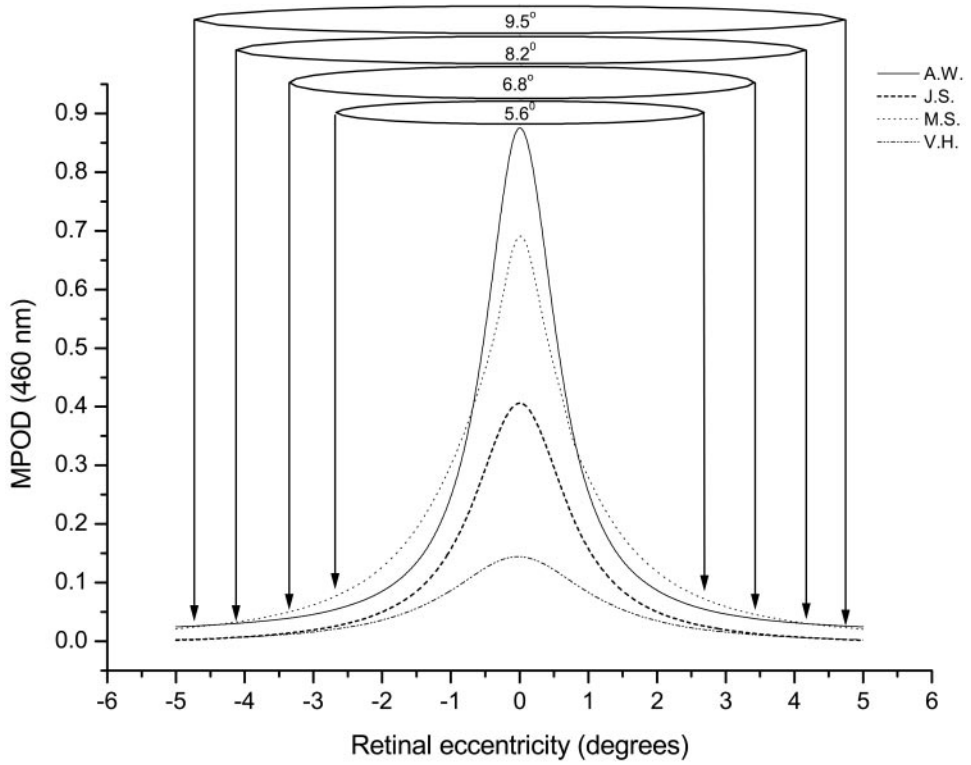

FIGURE 7. Lorentzian fits to spatial profiles of MPOD in all four subjects.

sizes, MP plays less of a mitigating role in PP. Admittedly, more subjects must be studied to address this hypothesis properly.

Convincing evidence that MP strongly attenuates PP is found in the results for experiment 3 (PP and retinal eccentricity). With the orange light (which spectrally avoids MP absorption), greater energy was needed in all four subjects, in a linear fashion, to elicit PP as retinal eccentricity increased (Fig. 5B). By contrast, the xenon-white light (partially screened by MP) produced functions dramatically different from the orange condition, especially for subjects AW and MS (Fig. 5A). For subjects AW and MS, essentially the *same* radiance level was necessary to induce PP for central viewing as for the 10° peripheral viewing condition. When all four subjects' data were analyzed statistically with a two-sample *t*-test, thresholds for central versus 10° viewing for the orange light condition were found to be significantly different ($t = 3.87$, $P = 0.008$). For xenon-white light, the two viewing conditions did not differ significantly ($t = 1.05$, $P = 0.33$). We propose that the discrepancy between the xenon-white and orange functions is due to the filtering effects of MP. In the central viewing condition, the 10° xenon-white stimulus was partially filtered by MP, whereas for the 10° eccentric viewing condition, the stimulus was imaged beyond the spatial extent of MP. For this reason, subjects AW and MS, who were shown to have considerably more MP than subjects JS and VH, tolerated substantially more xenon light in the central viewing condition than what would be dictated by a linear function. Presumably as a result of their MP levels, both AW and MS are shown to be equally sensitive to the xenon stimulus viewed 10° peripherally as viewed centrally. To a lesser extent (presumably due to less MP), subject JS was not able to tolerate as much light in the central viewing condition as subjects AW and MS, relative to 10° viewing. Finally, subject VH, who was shown to have very little MP, exhibited a nearly linear increase in PP threshold with eccentricity. The hypothesis that MP acts as a spatially integrated filter for PP is supported by these findings—subjects MS and AW had identical central/10° peripheral radiance ratios, yet quite different MPOD spatial profiles. As noted earlier in the article, the two subjects had identical spatially integrated MP levels, and this we assume to account for the identical radiance ratios. Given this result, a person with a large amount of MP may find intense lights in the periphery to be more disturbing relative to when they are viewed straight on.

The results of experiment 3 indicate that the PP response is preferentially biased to prevent the central retina from exposure to intense light of any spectral composition. Moreover, the results of Stringham et al.,[12] taken together with those of experiment 3 in the present study indicate that lights containing short-wavelength energy appear to be especially discomforting. In this regard, MP appears to act as a spatially integrated filter, serving to attenuate PP to a great extent. The logical and somewhat ironic implication of this idea is that people with high levels of MP would be able to withstand higher light levels without aversion (PP), thus exposing their anterior ocular media (e.g., lens) to more (potentially damaging) light. This conclusion is somewhat inconsistent with most of the current data, which suggest an inverse relationship between MPOD and lens optical density (for example, Ref. 29). Perhaps the carotenoid constituents of MP, lutein and zeaxanthin (which have been shown to exist in the lens[30]), may retard age-related increases in lens density, as suggested by Hammond et al.[31]

A Visual Pathway for PP

The present study provides data that are suggestive of the pathway that gives rise to the PP response. When the area versus radiance function for the orange-light condition is plotted against published values for parasol[32,33] and small bistratified[34] ganglion cell dendritic areas, the relationships are found to be strikingly similar (Fig. 8A). This correspondence suggests that spatial summation for PP is proportional to the dendritic field areas of parasol and small bistratified ganglion cells. This plot assumes that ganglion cell dendritic areas are radially symmetric about the fovea. This is true in the superior, temporal, and inferior retina, whereas the nasal retina's ganglion

Downloaded from iovs.arvojournals.org on 06/13/2021

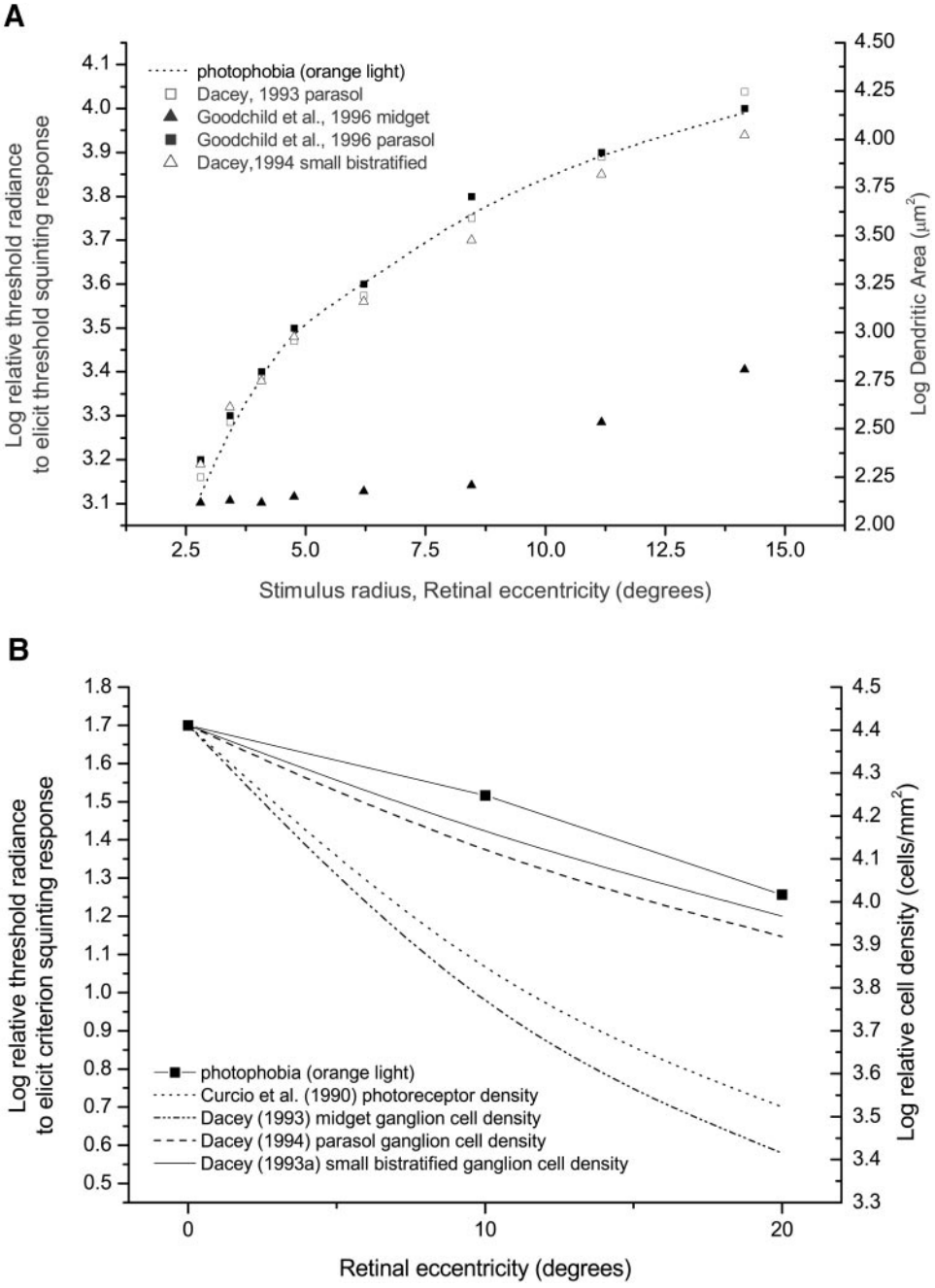

FIGURE 8. **(A)** Log relative sensitivity (1/threshold radiance) for PP to orange light (subjects' averaged data) plotted as a function of stimulus radius. Average log dendritic field areas of midget,[32] parasol,[31,32] and small bistratified[33] ganglion cells plotted for comparison. PP function is the least-squares fit to parasol and small bistratified data. **(B)** Log relative sensitivity (1/threshold radiance) for PP to orange light (subjects' averaged data) plotted as a function of temporal retinal eccentricity. Log relative spatial densities of photoreceptors,[35] midget ganglion cells,[31] parasol,[36] and small bistratified ganglion cells[33] plotted for comparison. All functions normalized to the peak sensitivity value for PP.

cell dendritic areas, at corresponding eccentricities, are slightly smaller.[35] The data derived from the orange light condition were chosen to compare with the ganglion cell dendritic area, because they appeared to be less affected by the complicating factors of MP than those derived from the white-light condition. The dendritic areas of midget ganglion cells are plotted for comparison and are found to be quite different from the PP, parasol dendritic area, and small bistratified dendritic area plots. The close correspondence of parasol and small bistratified ganglion cell dendritic areas to PP spatial summation suggests that PP could be mediated by parasol and small bistratified ganglion cells. Despite the very good fit to the area versus radiance data for the orange-light condition, the *areas* of parasol and small bistratified ganglion cell dendritic fields may not tell the complete story. In experiment 3, which assessed PP as a function of retinal eccentricity, it was found that the threshold for PP increased with eccentricity. It could be that the *spatial density* of ganglion cells or photoreceptors is related to the changes in PP sensitivity with eccentricity. To examine this possibility, the average spatial densities of cone photoreceptors,[34] midget ganglion cells,[30] parasol ganglion cells,[35] and small bistratified ganglion cells[32] were plotted for regions corresponding to the eccentricity data derived from PP to orange light (Fig. 8B). It can be seen that the spatial densities for all cells decreased with eccentricity. The parasol and small bistratified ganglion cell spatial densities, however, appeared to decrease in a fashion commensurate with the averaged orange PP sensitivity function. This finding supports further the hypothesis that PP is mediated through parasol and small bistratified ganglion cells. This notion is speculative, however, in that we did not directly assess our subjects' parasol, midget, or small bistratified ganglion cell receptive field areas and densities, but rather used published values for humans. Undoubtedly, there is some variability among individuals in this regard.

Downloaded from iovs.arvojournals.org on 06/13/2021

Two primary and well-understood parallel visual pathways (referred to as parvo- and magnocellular) remain segregated until late stages of cortical processing.[36] It has been well established that midget ganglion cells serve the parvocellular visual stream, and parasol ganglion cells serve the magnocellular visual stream.[37,38] Further, detailed experiments by Livingstone and Hubel[39] and Croner and Kaplan,[40] among others, have characterized specific functions of these two visual pathways. Generally, the parvocellular pathway has been shown to be involved in processing color, fine texture, and high spatial frequencies, whereas the magnocellular pathway is involved in processing luminance, motion, and low spatial frequencies.[36] Magnocellular cells have been shown to be exquisitely sensitive to small changes in luminance and luminance contrast.[41] Moreover, magnocellular cells have been shown to respond much more vigorously to changes in contrast (greater contrast gain) than their parvocellular counterparts.[40] These functional specialties are consistent with a mechanism that could give rise to PP and lend support for the idea that PP is mediated by the magnocellular pathway.

Small bistratified ganglion cells, as their name suggests, exhibit dendrites that stratify at two different levels in the inner plexiform layer.[42] They project to koniocellular sublayers K_3 or K_4 of the parvocellular region of the lateral geniculate nucleus (LGN). Relay cells from the LGN serving this pathway project to a subset of the cytochrome oxidase (CO) blobs found in layer 3B of striate cortex. The CO blobs have been shown to be essential for processing color vision.[36] It has been determined that small bistratified ganglion cells are the morphologic substrate of the "blue-on, yellow-off" cell.[42] Indeed, the inner "on" arbor of the small bistratified cell receives input from approximately 3 S-cone bipolar cells, whereas the outer "off" arbor receives input from one of two types of diffuse bipolar cell, which receive from a mixture of approximately 20 M- and L-cones.[42] Therefore, the role of the small bistratified ganglion cell in its contribution to PP could be one of spectral sensitivity. The relatively high PP sensitivity to short-wavelength light could be explained by the small bistratified cell's "blue-on" configuration. Perhaps the parasol and small bistratified ganglion cells act additively to signal visual discomfort. It follows that, as more short-wavelength light is introduced, PP would be more readily induced.

This hypothesis does not take into account a role for the rod photoreceptors in contributing to PP. There is some evidence, however, that indicates that rods may have a role to play in visual discomfort. That the rods are often the primary functioning photoreceptor at the onset of PP could suggest a rod-mediated mechanism. In addition, in the special case of rod monochromats (individuals lacking cones), it is well documented that PP is experienced under moderate lighting conditions.[43]

Conclusions

The primary finding of these experiments is that PP exhibits spatial summation for centrally viewed stimuli. In addition, for long-wavelength light, the PP threshold was found to increase substantially with increases in retinal eccentricity. For xenon-white light, however, subjects with relatively high MP levels exhibited an attenuation of PP for central viewing, relative to 10° eccentricity. The results of the present study support and extend the hypothesis that the PP response is preferentially biased to prevent the central retina from exposure to potentially damaging short-wavelength light. In this regard, PP could be considered, after MP, to be the second line of defense against retinal damage from visible short-wave light. Both PP and MP therefore appear to serve the function of foveal phototoprotection. PP presumably serves to protect extrafoveal and peripheral areas of the retina as well.

Acknowledgments

The authors thank Rob Drugan, Bill Stine, Max Snodderly, and Win Watson for their insightful comments and guidance.

References

1. Lebensohn JE. Photophobia: mechanism and implications. *Am J Ophthalmol*. 1951;34:1294–1300.
2. Kawasaki A, Purvin VA. Photophobia as the presenting symptom of chiasmal compression. *J Neuroophthalmol*. 2002;22:3–8.
3. Gutrecht JA, Lessell IM. Photophobia in trigeminal neuralgia. *J Neuroophthalmol*. 1994;14:122–123.
4. Eckhardt B, McClean JM, Goodell H. Experimental studies on headache: the genesis of pain from the eye. *J Nerve Ment Dis*. 1943;23:209–227.
5. Drummond P. A quantitative assessment of photophobia in migraine and tension headache. *Headache*. 1986;26:465–469.
6. King V. Discomfort glare from flashing sources. *J Am Optom Assoc*. 1972;43:53–56.
7. Lebensohn JE. The nature of photophobia. *Arch Ophthalmol*. 1934;12:380–390.
8. Howarth P, Heron G, Greenhouse D, Bailey I, Berman S. Discomfort from glare: the role of pupillary hippus. *J Illum Eng*. 1993;25:37–42.
9. Wirtschafter JD, Bourassa CM. Binocular facilitation of discomfort with high luminances. *Arch Ophthalmol*. 1966;75:683–688.
10. Vanagaite J, Pareja JA, Storen O, White LR, Sanc T, Stovner LJ. Light-induced discomfort and pain in migraine. *Cephalalgia*. 1997;17:733–741.
11. Vanagaite-Vingen J, Stovner LJ. Photophobia and phonophobia in tension-type and cervicogenic headache. *Cephalalgia*. 1998;18:313–318.
12. Stringham JM, Fuld K, Wenzel AJ. Action spectrum for photophobia. *J Opt Soc Am A Opt Image Sci Vis*. 2003;20:1852–1858.
13. Ham WT, Mueller HA, Sliney DH. Retinal sensitivity to damage from short wavelength light. *Nature*. 1976;260:153–155.
14. Gorgels T, van Norren D. Ultraviolet and green light cause different types of damage in rat retina. *Invest Ophthalmol Vis Sci*. 1995;36:851–863.
15. Rijsdijk, JP, Kroon, JN, van der Wildt, GJ. Contrast sensitivity as a function of position on the retina. *Vision Res*. 1980;20:235–241.
16. Scholtes A, Bouman MA. Psychophysical experiments on spatial summation at threshold level of the human peripheral retina. *Vision Res*. 1976;17:867–873.
17. Lie I. Visual detection and resolution as a function of retinal locus. *Vision Res*. 1980;20:967–974.
18. Cornsweet TN. Determination of the stimuli for involuntary drifts and saccadic eye movements. *J Opt Soc Am A Opt Image Sci Vis*. 1956;46:987–998.
19. Glezer VD. The receptive fields of the retina. *Vision Res*. 1965;5:497–525.
20. Yates SK, Brown, WF. Light-stimulus-evoked blink reflex: methods, normal values, relation to other blink reflexes, and observations in multiple sclerosis. *Neurology*. 1981;31:272–281.
21. Wooten BR, Hammond BR, Land RI, Snodderly DM. A practical method for measuring macular pigment optical density. *Invest Ophthalmol Vis Sci*. 1999;40:2481–2489.
22. Snodderly DM, Hammond BR. In vivo assessment of nutritional and environmental influences on human ocular tissues: lens and macular pigment. In: Taylor A, ed. *Nutritional and Environmental Influences on Vision.* Boca Raton, FL: CRC Press; 1999.
23. Werner JS, Donnelly SK, Kliegl R. Aging and human macular pigment density. *Vision Res*. 1987;27:257–268.
24. Hammond BR, Wooten BR, Snodderly DM. Individual variations in the spatial profile of macular pigment. *J Opt Soc Am A Opt Image Sci Vis*. 1997;6:1187–1196.
25. Chen SF, Chang Y, Wu JC. The spatial distribution of macular pigment in humans. *Curr Eye Res*. 2001;23:422–434.

Downloaded from iovs.arvojournals.org on 06/13/2021

26. Ciulla TA, Curran-Celentano J, Cooper DA, et al. Macular pigment optical density in a Midwestern sample. *Invest Ophthalmol Vis Sci*. 2001;108:730–737.
27. Bouman MA, van der Velden HA. The two-quanta explanation of the dependence of the threshold values and visual acuity on the visual angle and the time of observation. *J Opt Soc Am A Opt Image Sci Vis*. 1947;37:908–919.
28. Pirenne MH, O'Doherty EF. Individual differences in night-vision efficiency. *P.R. Spec Rep Ser Med Res Coun.* London: Chapman & Hall; 1957:294. Taken from: *Woodworth and Schlosberg's Experimental Psychology*. Austin, TX: Holt, Rinehart, & Winston; 1971.
29. Berendschot T, Broekmans, W, Klopping-Ketelaars, I, Kardinaal, A, van Poppel, G, van Norren, D. Lens aging in relation to nutritional determinants and possible risk factors for age-related cataract. *Arch Ophthalmol*. 2002;120:1732–1737.
30. Yeum KJ, Taylor A, Tang G, Russell RM. Measurement of carotenoids, retinoids, and tocopherols in human lenses. *Invest Ophthalmol Vis Sci*. 1995;36:2756–2761.
31. Hammond BR Jr, Wooten BR, Snodderly DM. Density of the human crystalline lens is related to the macular pigment carotenoids, lutein and zeaxanthin. *Optom Vis Sci*. 1997;74:499–504.
32. Dacey DM. The mosaic of midget ganglion cells in the human retina. *J Neurosci*. 1993;13:5334–5355.
33. Goodchild AK, Ghosh KK, Martin PR. Comparison of photoreceptor spatial density and ganglion cell morphology in the retina of human, macaque monkey, cat, and the marmoset *callithrix jacchus. J Comp Neurol*. 1996;366:55–75.
34. Dacey DM. Morphology of a small-field bistratified ganglion cell type in the macaque and human retina. *Vis Neurosci*. 1993a;10:1081–1098.
35. Watanabe M, Rodieck RW. Parasol and midget ganglion cells of the primate retina. *J Comp Neurol*. 1989;289:434–454.
36. Hubel DH. *Eye, Brain, and Vision.* New York, NY: Scientific American Library, No. 22; 1995.
37. Blasdel GG, Lund JS. Termination of afferent axons in macaque striate cortex. *J Neurosci*. 1983;3:1389–1413.
38. Rodieck RW. The primate retina. In: Steklis HD, Erwin J, eds. *Comparative Primate Biology*. Vol. 4. New York: Alan R. Liss, Inc. 1988:203–278.
39. Livingstone MS, Hubel DH. Segregation of form, color, movement, and depth: anatomy, physiology, and perception. *Science*. 1988;240:740–749.
40. Croner LJ, Kaplan E. Receptive fields of P and M ganglion cells across the primate retina. *Vision Res*. 1994;35:7–24.
41. Kaplan E, Shapley RM. The primate retina contains two types of ganglion cells, with high and low contrast sensitivity. *Proc Natl Acad Sci USA*. 1986;83:2755–2757.
42. Dacey DM, Lee BB. The blue-ON opponent pathway in primate retina originates from a distinct bistratified ganglion cell type. *Nature*. 1994;367:731–735.
43. Klingaman RL. Light adaptation in a normal and a rod monochromat: psychophysical and VEP increment threshold comparisons. *Vision Res*. 1979;7:825–829.

Downloaded from iovs.arvojournals.org on 06/13/2021